Modeling of Gas–Liquid Packed-Bed Reactors with Momentum Equations and Local Interaction Closures

ARTICLE *in* INDUSTRIAL & ENGINEERING CHEMISTRY RESEARCH · OCTOBER 2006

Impact Factor: 2.59 · DOI: 10.1021/ie0606338

4 AUTHORS, INCLUDING:

Ville Alopaeus
Aalto University
146 PUBLICATIONS **907** CITATIONS
SEE PROFILE

Katja Lappalainen
Aalto University
9 PUBLICATIONS **99** CITATIONS
SEE PROFILE

Mikko Tapani Manninen
VTT Technical Research Centre of Finland
37 PUBLICATIONS **593** CITATIONS
SEE PROFILE

Modeling of Gas−Liquid Packed-Bed Reactors with Momentum Equations and Local Interaction Closures

Ville Alopaeus,*,†,‡ Katja Hynynen,† Juhani Aittamaa,† and Mikko Manninen§

Laboratory for Chemical Engineering and Plant Design, Helsinki University of Technology, P.O.B. 6100, FIN-02015 HUT, Espoo, Finland, Chemical Engineering Laboratory, Aalborg University Esbjerg, Niels Bohrs Vej 8, DK-6700, Esbjerg, Denmark, and Process Chemistry, VTT, P.O.B. 1000, FI-02044 VTT, Finland

An algebraic model for the estimation of gas−liquid packed-bed hydrodynamic parameters is developed, based on one-dimensional material and momentum balances for gas and liquid phases. Underlying momentum exchange closures are critically analyzed, which leads to discarding some interaction models between the phases and development of new models based on local hydrodynamics. The present approach is based on more-relevant assumptions for the particle scale geometry than the slit models presented in the literature. The resulting model requires a one-parameter iterative solution, from which both pressure drop and liquid holdup are obtained. The model can be used without any extra complication in situations where the boundary conditions are specified either at the inlet or at the outlet of the reactor. It is suitable for modeling both low- and high-pressure operations, trickling as well as pulsing flow, upflow and downflow arrangements, and processes with Newtonian as well as non-Newtonian liquids. Finally, the present model is compared to its differential counterpart, and to available experimental data from open literature. Reasonably good agreement was observed for both pressure drop and liquid holdup data from a wide range of operating conditions, using only a single set of Ergun parameters.

Introduction

In gas−liquid packed-bed reactors, gas and liquid phases usually flow co-currently through a fixed bed of catalysts. Reactors of this type are commonly known as trickle-bed reactors. Co-current operation can be set up by either upward- of downward-flow arrangements, with downward flow being used more often, because of simpler control of the phases. In fixed-bed reactors, where the need to separate the catalyst from the reaction products is avoided, the co-current approach has been the most successful in practical installations. The specific advantages of a countercurrent flow arrangement are related to equilibrium-limited reactions and cases where feed contains harmful impurities to the catalyst. In co-current operation, the operating window for gas and liquid flow rates is much higher, compared to the countercurrent arrangement, because flooding is not a concern. This allows higher flow rates, which, in turn, improves mass-transfer characteristics between gas and liquid, and at the catalyst surface. A further benefit is a more-even distribution of gas and liquid phases in the bed, compared to the countercurrent flow, although usually at the expense of a greater pressure drop. However, because most industrial trickle-bed reactors (e.g., hydrogenation reactors) operate at high pressures, the pressure drop at a single catalyst bed is usually unimportant for the process economy. Nevertheless, a sufficiently accurate prediction of pressure drop and liquid holdup is important for reliable process design.

The design procedure for industrial process equipment, including trickle-bed reactors, is usually iterative, including an initial screening phase, preliminary process design for cost estimates, and refined information related to the feed composition and flow rates, as well as product specifications, until a detailed design for each equipment is provided, along with precise heat and material balances. During this process, various levels of process models are needed. The most often used models are those implemented in flowsheet simulators, along with correlations that can be either included in the simulators or used separately to analyze various factors of the process. For trickle beds, the most important hydrodynamic parameters are pressure drop over the catalyst bed, gas and liquid holdups, and catalyst wetting.

In commercial flowsheet simulators, the available models for trickle-bed reactors are very limited. In the best cases so far, a plug-flow model can be used with chemical kinetics and gas−liquid equilibrium, along with a separate correlation for pressure drop. On the simplest modeling level, the approach taken in this work can be used for initial screening of process alternatives. In more-rigorous modeling cases, detailed closure models can be implemented in more-advanced modeling platforms, such as computational fluid dynamics (CFD) software or process flowsheeting programs with detailed thermodynamic, reaction kinetic, and mass-transfer models. Some of these closure models are also developed later in this work.

Because the design process is iterative itself, not to mention the solution of material balances of complicated chemical processes, the models are needed repeatedly during this process. Simple correlations are used most often for pressure-drop and feed-component conversions in the reactor. The reactor model in this design phase is typically a correlation that relates the feed-to-catalyst ratio to conversion, or it is a plug-flow reactor model. In most practical cases, this is also the most rigorous model used, although, lately, CFD analysis of gas−liquid reactors has become a viable tool.[1,2] Being computationally intensive, CFD analysis is not possible routinely during the reactor design process. Currently, it can be used to analyze the behavior of the final design in more detail. Another fact favoring research with simple models is that the phase interaction models in the simpler and more-complex (multidimensional) models

* To whom correspondence should be addressed. E-mail address: ville@alopaeus.tkk.fi.

† Laboratory for Chemical Engineering and Plant Design, Helsinki University of Technology.

‡ Chemical Engineering Laboratory, Aalborg University Esbjerg.

§ VTT.

10.1021/ie0606338 CCC: $33.50
Published on Web 10/25/2006

are usually similar. The development of the interaction models then can be performed at a simpler modeling level and used with a more-rigorous geometry.

Underlying Models for the Trickle Bed

The description of fluid dynamics within a trickle-bed reactor can be achieved by formulating mass and momentum balances for the gas and liquid phases. Although physical models based on empirical formulation for gas and liquid permeabilities have also been shown to give good results,[3] we believe that purely mechanistic models with geometric interpretations are preferable. Physical significance of various interaction terms is more explicit, and further elaboration of the closure models for various interactions is straightforward when mechanistic models are applied.

Assuming one-dimensional flow, steady-state operation, and no mass transfer between the phases, the material balances for gas and liquid phases, respectively, are

$$\frac{\mathrm{d}}{\mathrm{d}z}(\alpha\epsilon\rho_G u_G) = 0 \tag{1}$$

$$\frac{\mathrm{d}}{\mathrm{d}z}[(1-\alpha)\epsilon\rho_L u_L] = 0 \tag{2}$$

and the corresponding momentum balances are

$$\alpha\epsilon\frac{\mathrm{d}p}{\mathrm{d}z} + \frac{\mathrm{d}}{\mathrm{d}z}(\alpha\epsilon\rho_G u_G{}^2) = \epsilon F_G + \alpha\epsilon\rho_G g \tag{3}$$

$$(1-\alpha)\epsilon\frac{\mathrm{d}p}{\mathrm{d}z} + \frac{\mathrm{d}}{\mathrm{d}z}[(1-\alpha)\epsilon\rho_L u_L{}^2] = \epsilon F_L + (1-\alpha)\epsilon\rho_L g \tag{4}$$

Here, the interpenetrating continuum assumption is made,[4] so that any location in the particle interstices, no matter how small the length scale that is considered, can contain both gas and liquid without the need to specify the location of the gas/liquid interface. The bed structure also is not modeled in detail; however, all characteristic properties of the bed, such as void fraction and particle size, are assumed to be homogeneous properties, no matter how small the volume element of the bed that is considered. This assumption is also generally called the Eulerian−Eulerian approach. This is the underlying assumption for the momentum equations; however, the closure terms in these models can still be modeled based on the local geometry and flow details on a particle scale.

The assumption of one-dimensional plug flow is usually justified in large-scale packed beds, if feed and discharge details are properly designed. In the case of improper feed distribution, the closure models of this work can still be used; however, a more-complicated geometrical model is needed for the reactor. Steady state is a reasonable assumption, even in the cases of startup or shutdown, if only relatively slow transients are considered. Despite the assumption of no momentum transfer due to mass transfer, the model is applicable also in situations with moderate mass-transfer rates, because the rate of momentum transfer is often negligible in vaporization or condensation. Only in cases of considerable phase change should the momentum and material balances be appended by appropriate terms. This can be done in more-rigorous reactor models without losing the validity of the present model development. Turbulent convection of momentum is also neglected. A more-detailed description of the underlying material and momentum balances has been presented by Iliuta and Larachi.[5] In the following development, bed void fraction gradients are neglected, so that each of the balance equations (eqs 1−4) can be divided by ϵ.

Next, a linear pressure−density relation is assumed for the gas phase. Note that it is not necessary to retain the ideal gas law; however, in the case of a more-complicated equation of state, a constant compressibility factor in the modeled catalyst bed must be assumed in the following derivation. The density−pressure relation can then be written as

$$\rho_G = \frac{pM}{z_c RT} \tag{5}$$

where z_c is the compressibility factor that is assumed to be constant along the trickle bed. According to the prevailing assumptions, gas superficial flow (j_G) is not a constant, because the gas density varies along the bed height. In the case of a linear density−pressure assumption, it can be written as

$$j_G = \frac{j_{G0}p_0}{p} \tag{6}$$

To simplify the material and momentum balances, we first note that

$$u_L = \frac{j_L}{\epsilon(1-\alpha)} \tag{7}$$

$$u_G = \frac{j_G}{\epsilon\alpha} \tag{8}$$

The following equations for gas and liquid momentum balances then can be obtained:

$$\left(1 - \frac{\rho_{G0}j_{G0}{}^2p_0}{\alpha^2\epsilon^2p^2}\right)\frac{\mathrm{d}p}{\mathrm{d}z} - \frac{\rho_{G0}j_{G0}|j_{G0}|p_0\mathrm{d}\alpha}{\epsilon^2\alpha^3p}\frac{}{\mathrm{d}z} = \frac{F_G}{\alpha} + \frac{\rho_{G0}pg}{p_0} \tag{9}$$

$$\frac{\mathrm{d}p}{\mathrm{d}z} + \frac{\rho_L j_L|j_L|}{\epsilon^2(1-\alpha)^3}\frac{\mathrm{d}\alpha}{\mathrm{d}z} = \frac{F_L}{1-\alpha} + \rho_L g \tag{10}$$

This set of differential equations can be written, with a compact notation, as

$$\frac{\mathrm{d}(\alpha,p)^T}{\mathrm{d}z} = \mathbf{A}(\alpha,p)^{-1}\cdot\mathbf{b}(\alpha,p) \tag{11}$$

where **A** is the mass matrix that contains terms multiplying differentials in the previous set of equation and **b** is a column matrix of the right-hand sides of the equations. This set of equations can be solved with any off-the-shelf ordinary differential equation (ODE) solver. The same set of equations also applies for countercurrent reactors, where the gas-phase velocity takes negative values. In downflow arrangements, numerical values of superficial velocities and gravitational acceleration are of the same sign, whereas in upflow arrangements, either velocities or gravitational acceleration should be set as negative values.

The situation is more complicated than previously presented if there are also outlet boundary conditions along with inlet conditions. The most typical of such specifications is pressure, which can be specified either at the reactor inlet or at the outlet. If there are mixed boundary conditions including both inlet and outlet specifications, the set of equations needs to be solved iteratively using, for example, a shooting method. Another option is to solve profiles through the entire bed simultaneously, for example, through the use of various difference schemes.[6]

Closure Equations

For completely wetted catalyst particles, the possible interactions between phases are between liquid and solid phases, and

between gas and liquid phases. In the literature, the interactions are usually formulated separately between gas and solid and between gas and liquid. Some authors neglect the interaction between the gas and liquid phases by reasoning that trickling flow is the so-called "low interaction regime",[6−8] whereas others include this term into their models.[1,2,9−11] Because catalyst particles are assumed to be completely wetted in the hydrodynamic model presented here, all forces acting from gas to solid must act via the liquid phase. When the gas−solid and gas−liquid interactions are both included in the model, this also leads to an incorrect limiting one-phase pressure gradient in cases where the liquid phase is vanishing (in which case its velocity, relative to the particles, also approaches zero), whereas the pressure gradient is reduced to the correct value as the gas phase is vanishing. Therefore, only liquid−solid and gas−liquid interactions are considered here. For a partially wetted catalyst, both gas−liquid and gas−solid terms could be taken into account by weighting the appropriate drag terms by a factor that was dependent on catalyst wetting. The question related to the valid interaction regime should be resolved by appropriate gas−liquid flow models on the catalyst scale and, correspondingly, by appropriate friction coefficients, not whether gas acts directly to solid or via the liquid film. One attempt to resolve the problem is the double slit model,[12] which is a straightforward extension to the fully wetted slit model adopted here. Apparent success in the literature correlations formulated solely for gas−solid interaction while neglecting the gas−liquid component may result from the fact that the relative velocity between the gas and liquid phases is, in most cases, similar to the pure gas velocity. Use of an incorrect relative velocity in the gas-phase momentum balance may also explain some differences in the functional dependency of the friction terms on liquid saturation between downward and upward flow arrangements.[13]

The phase interactions encountered in the trickle beds can be expressed as a sum of viscous and inertial contributions. It is customary to write these equations in terms of superficial velocities, so that all effects related to the available pore space for fluid flow are lumped into the closure terms:

$$F_G = -f_{GL} = -\alpha(A_{GL}\mu_G j_r + B_{GL}\rho_G j_r|j_r|) \tag{12}$$

$$F_L = f_{GL} - f_{LS} = f_{GL} - (1-\alpha)(A_{LS}\mu_L j_L + B_{LS}\rho_L j_L|j_L|) \tag{13}$$

where j_r is the relative superficial velocity between gas and liquid. Its definition and significance is discussed later.

The most widely accepted form of phase interactions in porous media is expressed as the modified Ergun equations.[14] For gas−liquid flow, these can be expressed as

$$A_{LS} = E_{\mu LS}\frac{(1-\epsilon)^2}{(1-\alpha)^3\epsilon^3 d_p^2} \tag{14}$$

$$B_{LS} = E_{\rho LS}\frac{1-\epsilon}{(1-\alpha)^3\epsilon^3 d_p} \tag{15}$$

$$A_{GL} = E_{\mu GL}\frac{(1-\alpha\epsilon)^2}{\alpha^3\epsilon^3 d_p^2} \tag{16}$$

$$B_{GL} = E_{\rho GL}\frac{1-\alpha\epsilon}{\alpha^3\epsilon^3 d_p} \tag{17}$$

Some authors include a term for the gas-phase interaction closures that describe the increment in the apparent particle size due to liquid film at the surface.[9,10] Here, a different approach is taken, namely, that the tortuosities experienced by gas- and liquid-phase flows are assumed to be functions of gas saturation in the pores. Appropriate tortuosity models are developed later in this paper. The particle size correction has been omitted, because the liquid is assumed to reside mainly near the particle−particle contact points, rather than form a layer of constant thickness on particle surfaces.

The Ergun formulation is usually considered to include all porosity-related factors and gas/liquid saturation within pores, so that only the superficial velocities are used in the j terms. The relative superficial velocity between the gas and liquid phases is not defined as clearly as j_G and j_L. It is well-known that, for flow in ducts with periodic throats, the pressure drop is mainly confined in these throats. Fluid flow in packed beds can also be considered to follow similar trend. The geometry of these throats, among other topological parameters of the bed, is included in the Ergun constants, so that there is no need to model them separately in the interaction closures. However, for the gas−liquid relative velocity that appears in the interfacial drag formulation, the situation differs from this. Although liquid is assumed to reside preferably near the particle−particle contact points, in the case of completely wetted particles, these throats are probably narrower for gas flow than the bed average values would predict. The surface tension forces also have a tendency to strangulate narrow gas paths in the center of the throat, surrounded by a liquid film on the particle surfaces. Because the gas−liquid interaction is most probably confined in these throats, the gas velocity should be modified. It is assumed here that the gas velocity in these throats is $1/\alpha$ times higher than the bed average. This assumption gives better results, compared to the experimental data than using the bed average values. With this assumption, we end up with the following relative velocity expression:

$$j_r = \alpha\epsilon\left(\frac{u_G}{\alpha} - u_L\right) = \frac{j_G}{\alpha} - \left(\frac{\alpha}{1-\alpha}\right)j_L \tag{18}$$

Tortuosity Model for the Two-Phase Ergun Parameters. Originally, the Ergun parameters were postulated as being universal, having the numerical values $E_\mu = 150$ and $E_\rho = 1.75$. However, it has been shown in later reports that this is not the case.[7,15−19] Nemec and Levec[20] proposed an improvement to the original parameters using empirical functions for nonspherical particles, whereas the original values were retained for spherical particles. Several other parameter sets have been presented as well; for example, Kundu et al. proposed values of $E_\mu = 250$ and $E_\rho = 2.1$ specifically for spherical nonporous material, which is often used in laboratory experiments related to trickling flow.[19] Macdonald et al.[16] obtained values of $E_\mu = 180$ and $E_\rho = 1.8$ for the two parameters, based on somewhat larger experimental data than that used by Ergun. For rough particle surfaces, they suggested using a value of $E_\rho = 4$ for the inertial contribution. Iliuta and co-workers[18,21] proposed neural network models to improve the Ergun parameters for various bed configurations. Although their approach improves the original Ergun model in many cases, their procedure complicates the model application to some extent, and more than that, some physical insight may be lost when a huge set of neural network parameters are fitted to experimental data.

It seems that the one-phase Ergun parameters are quite strongly affected by the level of consolidation in the bed. For a certain particle shape and roughness, loose packing results in high parameter values, whereas a highly consolidated bed results

in low values. Generally, loose packing may be expected if the bed-to-particle diameter ratio is small, especially in cylindrical beds, and also for rough particles that do not slip into an ordered grid easily. This might be explained using a concept of "entropy" of the packed bed, i.e., for well-organized lattices, as in highly consolidated beds, the parameters have a tendency to be lower, because of a more-structured fluid flow field. Although the present model allows refining the one-phase Ergun parameter values, a single set of parameters is used in comparison to all datasets, so that the model is truly predictive.

According to the slit model of Holub,[22] the parameters can be calculated from

$$E_\mu = 72T^2 \tag{19}$$

$$E_\rho = 6f_\tau T^3 \tag{20}$$

where T is the tortuosity of the bed, which is a characteristic of the packing material and the packing method, and f_τ is a "friction factor" between the phases.

In this work, we adopt the Ergun parameters that have been proposed by Macdonald et al.[16], i.e., $E_\mu = 180$ and $E_\rho = 1.8$. From these values, the tortuosity and the friction factors are

$$T_0 = \sqrt{\frac{E_\mu}{72}} \approx 1.5811$$

$$f_\tau = \frac{E_\rho}{6\left(\frac{E_\mu}{72}\right)^{3/2}} \approx 0.075895$$

As speculated by Attou et al.,[10] the tortuous pattern generally is dependent on the gas and liquid volume fractions in the bed. Based on that idea, a phase-fraction-dependent tortuosity model is developed here. At the limit of single-phase flow (gas or liquid), the empty bed tortuosity given previously is used. In the intermediate region, a gas volume fraction dependency should be included in the model. Such dependency is developed here.

According to the slit model of Holub,[22] the slit angle and tortuosity are related as

$$T = \frac{1}{\cos\theta} \tag{21}$$

where θ is the angle of the slit. It is assumed here that the slit angle for liquid flow and the gas saturation have a simple relation, $\theta = (\pi/2)\alpha$, so that the volume fraction of liquid is mapped to a quadrant of a circle that describes the possible liquid slit angles (Figure 1). By combining the empty-bed value and the aforementioned development, the liquid-phase tortuosity is

$$T_L = \frac{T_0}{\cos\left(\frac{\pi}{2}\alpha\right)} \tag{22}$$

Note that, at the limit of vanishing liquid phase, the model predicts that the liquid-phase tortuosity approaches infinity. This is not in contradiction with experimental observations, where a significant amount of residual liquid is usually found. The present model actually helps to predict the presence of residual liquid (static holdup).

At the limit of the liquid-full bed (only narrow gas rivulets or separate bubbles at the center of the pores), gas tortuosity is assumed to approach the average of the value for one-phase flow and for a straight flow path, whereas liquid tortuosity approaches the empty-bed tortuosity. A linear dependency is assumed for the intermediate gas volume fractions as

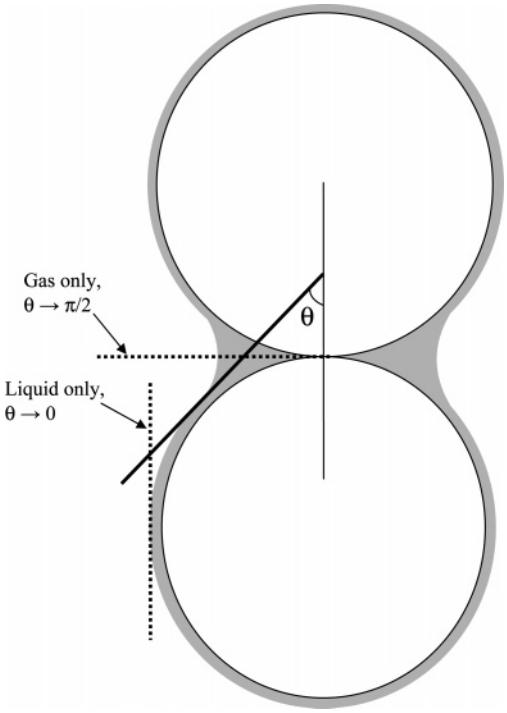

Figure 1. Schematic picture of the effect of liquid saturation on tortuosity. θ corresponds to the slit angle in Holub's (1990) model.

$$T_G = \frac{T_0 + 1}{2} + \alpha\left(\frac{T_0 + 1}{2} - 1\right) \tag{23}$$

These tortuosity functions are then used to update Ergun parameters for two-phase flow. Note that, according to the tortuosity models previously presented, the tortuosity experienced by the gas-phase flow is always less than the tortuosity of an empty bed, whereas the tortuosity for the liquid phase is always greater than the corresponding empty-bed value. This is in agreement with the underlying assumption that the liquid preferably flows along particles, whereas the gas flows at the particle interstices. This assumption is made in practically all phenomenological trickle-bed models presented in the literature. These detailed tortuosity models can be further refined in the future by small-scale experiments or by numerical simulation using the Volume-of-Fluid (VOF) or Lattice−Boltzmann methods.

Pulsing Flow. If the reactor operates in pulsing mode, the liquid-phase tortuosity is expected to increase. Holub[22] analyzed the onset of pulsing using Kapiza's stability criterion for surface waves of liquid flow on an inclined surface. The flow is expected to be unstable if

$$P = \frac{Re_{L,crit}\Psi_L^{1/11}E_\mu^{5/11}}{25Ka^{1/11}} > 1 \tag{24}$$

where $Re_{L,crit}$ is the critical Reynolds number for pulsing ($Re_{L,crit} = \rho_L j_L d_p/[\mu_L(1-\epsilon)]$), Ψ_L is the dimensionless body force acting on the liquid ($\Psi_L = 1 - (1/\rho_L g)(dp/dz)$), and Ka is the Kapiza number ($Ka = \sigma^3\rho_L/\mu_L{}^4 g$). The single-phase value $E_\mu = 180$ is used to keep the model consistent with the analysis of Holub.[22]

Here, this stability criterion is extended to describe the increased liquid-phase tortuosity by a simple linear expression,

$$\xi_P = 1 + a_p(P - 1)\alpha(1 - \alpha) \qquad (\text{if } P > 1) \qquad (25)$$

so that $T_{L,pulsing} = T_L\xi_P$. The term $\alpha(1 - \alpha)$ accounts for the available void for the pulses and forces the pulsing correction to unity in the case of single-phase flow.

Because the pulsing criterion requires knowledge of the dimensionless pressure drop, it must be estimated either iteratively or, preferably, through the use of a predictor−corrector scheme (presented later in this paper).

Capillary Forces. In systems with large interfacial tension and slow velocities, capillary forces affect permeabilities. This is also a reasonable explanation for a relatively flat pressure drop−velocity curve in many experiments, where a two-phase pressure drop seems to be considerably higher than corresponding predicted values, especially for very low velocities of either phase. Here, a correction is proposed, based on an idea that when the capillary number, $Ca = \mu j/\epsilon\sigma$, is low, stagnant gas or liquid pockets remain in the porous media, leading to a partially blocked void structure for the bulk flow. For the liquid phase, this corresponds to a situation where an interstitial void is completely filled by liquid, and the gas−liquid surface resides at the void entrance throats, preventing gas from intruding into the void. For the gas phase, the situation may be depicted as a bubble trapped inside a void, where surface tension prevents the bubble from squeezing through the next throat. To describe this, the following empirical forms are developed for effective pore volumes for gas and liquid phases, respectively:

$$\epsilon_{eff,G} = \epsilon - \epsilon_s \exp(-a_c Ca_L) \qquad (26)$$

$$\epsilon_{eff,L} = \epsilon - \epsilon_s \exp(-a_c Ca_G) \qquad (27)$$

These values are then used in the closure models described by eqs 14 and 15 and eqs 16 and 17 for the gas- and liquid-phase terms, respectively. Note that the liquid-phase capillary number affects the gas-phase effective porosity and vice versa. In cases of stagnant liquid operation, Ca_L takes a value of zero, and the available void fraction for gas-phase flow is, correctly, the total void minus static holdup, $\epsilon - \epsilon_s$.

For the static holdup, the following correlation is used in this work:

$$\epsilon_s = \frac{1}{20 + 0.9Eo^*} \qquad (28)$$

where

$$Eo^* = \frac{\rho_L g d_p^2 \epsilon^2}{\sigma(1 - \epsilon)^2} \qquad (29)$$

is the modified Eötvös number, as proposed by Saez and Carbonell.[7]

Chatzis and Morrow[23] studied the removal of trapped residual oil in sandstones, and they determined that the critical capillary number value for the mobilization was 2×10^{-5}. If an 1% effect of the capillary forces on liquid saturation is assumed at the limiting value, the parameter a_c takes a value of $-\ln(0.01)/(2 \times 10^{-5}) \approx 230\,000$. This value is used in this work.

The previously described capillarity phenomenon is important, mainly when flow rates are relatively low. In industrial trickle-bed reactors, correction for the voidage can often be neglected; however, in the interpretation of some laboratory data, the correction is applicable. One should also keep in mind that bed-wide correlations based on capillary forces have only limited physical significance. Capillary forces and particle wetting possess hysteretic behavior, especially on rough surfaces.[24] This has been observed also experimentally in trickle-bed reactors.[25] The capillary phenomenon is also a complicated function of particle interstitial void and throat structure and size distribution between the particles within trickle-bed reactors, so that the exact parameter values for effective voidage are not only time-dependent but also bed-structure-dependent.

One interesting observation is that, in practically all capillary-related models developed for trickle-bed reactors, only the gas−liquid surface tension is considered. For liquid wetting on solid surfaces, the net effect of surface tension between gas−solid and liquid−solid interactions is more important, because they are related directly to the wettability characteristics of the solid surface. Actually, the gas−liquid surface tension does not even contribute to the qualitative behavior of whether the liquid preferably distributes on the surface or recedes as isolated droplets.[24] Naturally, the gas−liquid surface tension strongly affects the capillary phenomenon; however, it seems that, at the moment, most capillary models that are applied to trickle-bed modeling lack the effect of solid-phase surface properties.

Non-Newtonian Liquids. For non-Newtonian liquids, perhaps the first assumption in the interpenetrating continua momentum equation approach is just to use the apparent liquid viscosity in the momentum closure equations. The shear rate in the packed bed then must be estimated for models that involve liquid viscosity. We propose here to use the wall shear rate from pipe flow analogy,[26] but with the particle diameter as the characteristic length, and actual liquid interstitial velocity. This gives the shear rate as

$$\gamma = \frac{8u_{ave}}{d} = \frac{8j_L}{(1 - \alpha)\epsilon d_p} \qquad (30)$$

Then, for example, the Ostwald de Waele (OdW) model gives

$$\mu = k\left(\frac{8j_L}{(1 - \alpha)\epsilon d_p}\right)^{n-1} \qquad (31)$$

where k and n are OdW viscosity model parameters. In the Numerical Examples section, we have used the OdW model, but any other generalized Newtonian model with shear-rate-dependent viscosity also can be used.

Algebraic Formulation

Although the one-dimensional formulation for continuity and momentum balances is relatively straightforward to solve, there is clearly a need for an even-simpler model that can be used similarly for algebraic correlations.[27] In this chapter, some assumptions are made to the ODEs to obtain such a model.

If the relative significance of various terms of the momentum equations is examined, it can be noticed that the terms including phase fraction gradients are negligible, compared to the other terms. This can also be observed by comparing the momentum convection terms to the inertial component of the interaction terms in the momentum equations. Here, the analysis is conducted only for the inertial component in the gas phase; however, similar reasoning can be applied for the viscous friction term in the gas phase and for the liquid-phase terms as well.

If we assume, only for the order-of-magnitude analysis of various terms in the momentum equation, that $j_r \approx j_G$, the ratio of convection to inertial friction in the gas-phase reduces to

$$\frac{\text{convection of momentum}}{\text{friction due to inertia}} = \frac{d_p(\mathrm{d}(\alpha\epsilon\rho_G)/\mathrm{d}z)}{\alpha\epsilon\rho_G}\frac{\alpha\epsilon}{E_{\rho GL}(1-\alpha\epsilon)} \quad (32)$$

The first part of the equation is equal to the relative change of the gas "superficial density" (gas mass divided by total bed volume) over a distance of one particle diameter. This change is much below unity in all cases relevant to trickle-bed reactors, perhaps excluding porous region surfaces, where there is a sudden change in porosity. Because the second part is also less than unity (if $\alpha\epsilon < E_{\rho GL}/(1 + E_{\rho GL})$, as it usually is), it can be concluded that the ratio of the two terms is usually very small and, therefore, the convection term can be neglected in the momentum equations. This approach has been adopted in most phenomenological pressure drop correlations.[8,21] (See also Choudhary et al.[28] for further discussion about the relevance of the inertial term.)

The momentum equations then can be written in the following form:

$$\frac{\mathrm{d}p}{\mathrm{d}z} = \frac{F_G}{\alpha} + \rho_G g \quad (33)$$

$$\frac{\mathrm{d}p}{\mathrm{d}z} = \frac{F_L}{(1-\alpha)} + \rho_L g \quad (34)$$

Because the pressure gradients calculated from the gas and liquid phases must be equal in the absence of surface forces, we have two equations and two unknowns, namely, the pressure gradient and the gas-phase interstitial volume fraction. By equating the pressure gradients for the gas and liquid phases, a single equation for the gas volume fraction can be obtained. Although nonlinear, it can be solved rather easily, after which the pressure gradient is obtained from either of the previous equations.

Predictor−Corrector Scheme for Variable Density and Pulsing Flow

In the algebraic formulation, the easiest and most robust way to solve the equation for volume fraction is to assume constant friction terms along the reactor bed. For high-pressure operations, where pressure drop is small, compared to the total pressure, this is a reasonable assumption, whereas for low-pressure and vacuum operations, the gas-phase density and, correspondingly, the friction factors can change considerably along the bed height. In that case, some effective bed-average values for the gas-phase density and friction factors should be used in the algebraic approach. Hence, a further correction is introduced, based on variable gas-phase density. Here, the correction is based on the pressure drop calculated from the momentum equation for gas phase, because the liquid-phase momentum equation is altered to a greater extent by the pulsing correction shown below.

The bed-average gas-phase density is calculated by first estimating the pressure at the outlet:

$$p_1 = p_0 + h\left(\frac{\mathrm{d}p}{\mathrm{d}z}\right) = p_0 + h\left(\frac{-f_{GL}}{1-\alpha} + \rho_L g\right) \quad (35)$$

If the outlet pressure is given, the previous equation should be solved for the inlet pressure, p_0.

Although a simple arithmetic average of the densities at the inlet and outlet pressures produces relatively good results for the bed-average effective density, a weighted average, $\rho_G = (\rho_0 + \lambda\rho_1)/(1 + \lambda)$, is still better, giving

$$\rho_G = \frac{\rho_0}{1+\lambda}\left[1 + \lambda\left(\frac{p_1}{p_0}\right)\right]$$

(if inlet pressure is specified, along with density (ρ_0))

and

$$\rho_G = \frac{\rho_0}{1+\lambda}\left(\frac{p_0}{p_1} + \lambda\right)$$

(if outlet pressure is specified, along with density (ρ_0)) (36)

In these equations, p_1 is the outlet pressure and p_0 is the inlet pressure, one of which is estimated based on constant friction terms. In the following development, we have used $\lambda = 1.5$.

Another closure model where the pressure drop appears is the tortuosity model in the pulsing regime. To avoid two-parameter iteration (pressure drop, in addition to the gas saturation), the predicted pressure drop presented above can be used to calculate the pulsing regime liquid tortuosity. The dimensionless pressure drop is first predicted from

$$\Psi_L = \frac{f_{GL}}{\alpha\rho_L g} + 1 - \frac{\rho_G}{\rho_L} \quad (37)$$

and the updated tortuosity for the liquid phase is then calculated from eq 25.

After the predictor step, the updated average density should be used to recalculate the average gas-phase superficial velocity, the average relative velocity between gas and liquid, and the friction terms presented earlier. The liquid-phase momentum source term is recalculated in the view of the tortuosity models (eqs 19 and 20) as

$$F_L = f_{GL} - f_{LS} = f_{GL} - (1-\alpha)(A_{LS}\xi_P^{\,2}\mu_L j_L + B_{LS}\xi_P^{\,3}\rho_L j_L|j_L|) \quad (38)$$

For simplicity, these corrections are applied only once in the present development during each iteration step of the algebraic model. A more rigorous approach would require iteration of both the gas saturation and the pressure drop, in which case the estimated pressure drop at each iteration could be used in the tortuosity closures for pulsing flow.

Summary of the Modeling Steps

The following steps summarize the solution of the present model. Given (i) the pressure at the inlet or at the outlet of the bed, (ii) the gas and liquid superficial flow rates, (iii) the physical properties for gas and liquid at inlet conditions (densities, viscosities, and surface tension), and (iv) the packing properties (particle size, void fraction), the solution algorithm is then described by the following steps:

(1) Calculate the effective interstitial void available for the gas and liquid, based on capillary force correction (eqs 26 and 27).

(2) Guess the initial value for the gas saturation. The exact value of the initial estimate is usually not very important; 0.5 is good for most cases.

(3) If liquid is non-Newtonian, calculate the effective viscosity using the shear rate from eq 30.

(4) Calculate tortuosities from eqs 22 and 23.

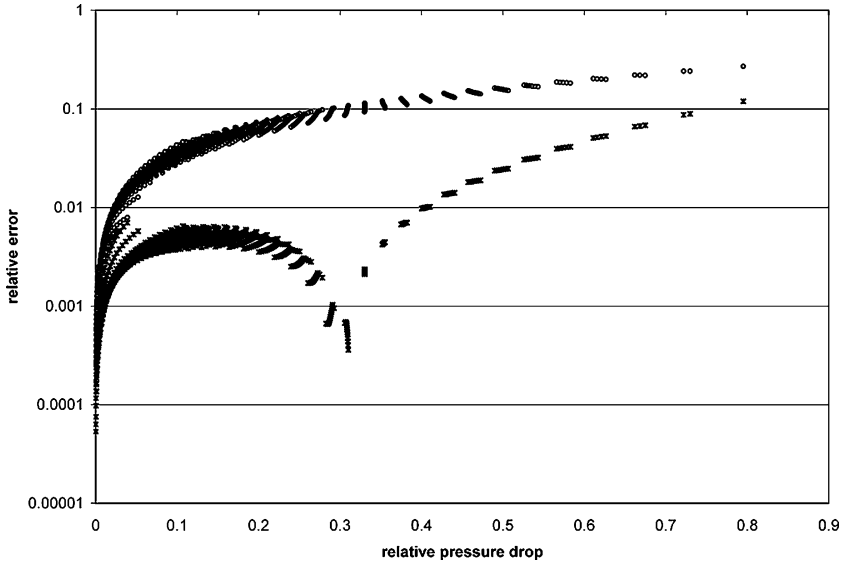

Figure 2. Relative error when algebraic model is used compared to the differential model. Circle symbol (○) refers to the constant density case, and cross symbol (×) refers to the corrected density case.

(5) Calculate phase-dependent Ergun parameters from eqs 19 and 20.

(6) Calculate the closure terms, using eqs 14−17.

(7) Calculate phase interactions, eqs 12 and 13 and correct for gas density from eqs 35 and 36.

(8) Calculate the pulsing parameter (using eqs 37, 24, and 25) and correct for pulsing (using eq 38).

(9) Calculate the pressure drops for the gas and liquid phases from eqs 33 and 34. If not equal, go to step 2.

(10) When the estimated pressure drops from eqs 33 and 34 are equal, the model is solved. Final gas saturation from the last guessed value gives the phase fractions. The pulsing parameter gives an estimate for the flow regime.

Numerical Examples

Comparison of the Differential and Algebraic Formulations. First, the assumptions behind the derivation of the algebraic model were verified numerically. The following input values were used in the comparison, corresponding to air−water system in atmospheric pressure and room temperature: $\rho_L = 998.2$ kg/m^3; $\rho_{G0} = 1.22649$ kg/m^3; $\mu_L = 0.001003$ kg/(m s); $\mu_G = 1.7894 \times 10^{-5}$ kg/(m s); $\epsilon = 0.368$, $h = 1$ m, $d_p = 3$ mm, and $\sigma = 0.0719$ N/m.

The gas and liquid inlet velocities were varied independently, from 0.003 m/s to 0.5 m/s (gas phase) and from 0.00006 m/s to 0.01 m/s (liquid phase) with geometric series increments. Thirty different values were set for both variables, so that a total of 900 points were calculated. With the highest relative pressure drops (∼0.8), the gas velocity profiles within the reactor were strongly curved as the pressure level decreases and the gas volumetric flow increases toward the end of the reactor. Using the result from the algebraic solution as an initial value for the integration, the number of integration steps at the vicinity of the inlet was greatly reduced, leading to faster solution of the model. Therefore, we suggest using the algebraic solution as the inlet boundary condition also for those cases where the model is solved using a more-rigorous reactor model.

In all tested cases, the gas volume fraction from the algebraic model was between the minimum and maximum values along the bed length, as predicted by the differential model. The maximum and minimum estimated interstitial gas fractions were between 0.25 and 0.87.

Figure 2 compares the differences between the modeled pressure drops with the two methods. It can be observed that the relative error is increased as the relative pressure drop increases. If the correction is applied, errors are usually an order of magnitude smaller than that calculated with the constant gas density. Because the density correction is only a single algebraic equation and does not complicate the structure of the equation to be solved, we recommend using it in all cases.

Comparison to the Literature Data and Available Correlations. In the next step, the model developed in this paper was compared to the available literature data. Both low- and high-pressure data were collected, including data from the trickle and pulse regions, and upflow and downflow arrangements, and experiments with both Newtonian and non-Newtonian liquids. So far, only co-current flow data were collected; however, the model has the potential to model countercurrent arrangements also. The countercurrent data is much sparser for trickle-bed reactors than for packed-separation columns, such as that in distillation or absorption. The packed-column data would require separate analysis of the phase interactions, and this is outside the scope of this work.

There are two possible configurations for experiments with no gas feed. The first is to keep the bed open to the same pressure at both ends. In this case, liquid flow drags some gas through the bed. The gas flow rate then should be iterated simultaneously with the liquid holdup, using the criterion that the pressure drop is zero, from both eqs 33 and 34. This leads to a different model structure than that in gas−liquid flow cases. Therefore, the other option is used, namely, that the upper end of the bed is closed, so that its pressure will be slightly below the atmospheric pressure, and, correspondingly, the gas flow is exactly zero. In most practical cases, the difference between the two formulations is negligible. The pulsing correction was neglected in cases of no gas flow.

Pressure drop and liquid holdup data were compared to model predictions. In cases where static liquid holdup was not given, the correlation by Saez and Carbonell (eq 28) was used in the conversion of dynamic holdup to total holdup values. Note that, in the actual reactor, there is no separate liquid volume that belongs to the static or dynamic holdup. In the laboratory measurements, total holdup is far more difficult to measure accurately than dynamic holdup, and, therefore, a correlation

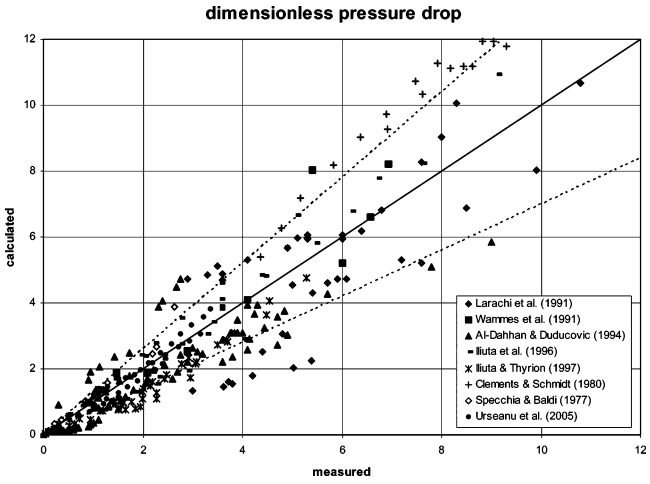

Figure 3. Parity plot of calculated and measured dimensionless pressure drops $dp/d(z\rho_L g)$. Dashed lines correspond to ±30% relative errors.

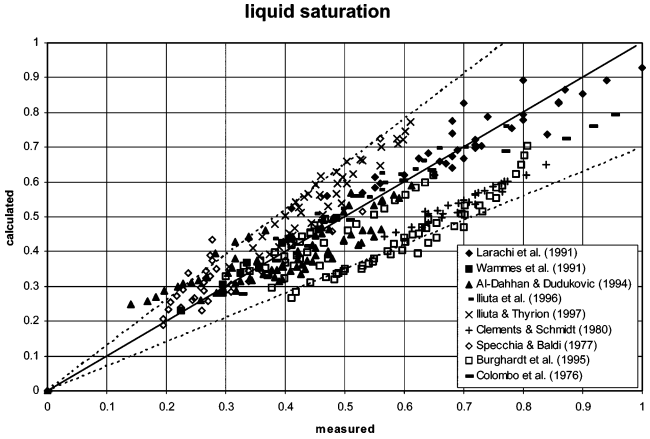

Figure 4. Parity plot of calculated and measured liquid saturations. Dashed lines correspond to ±30% relative errors.

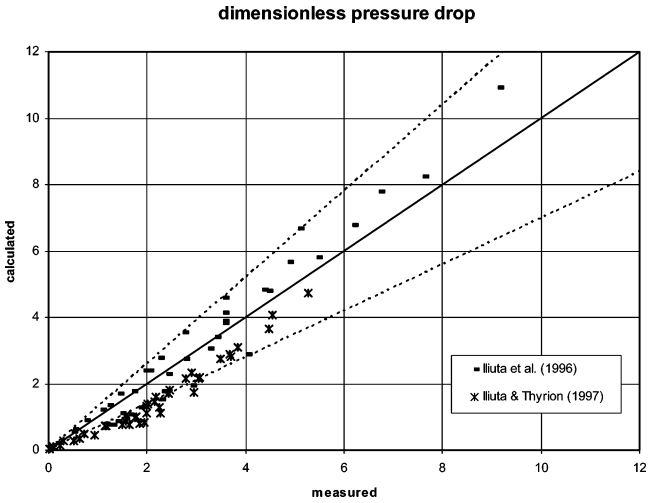

Figure 5. Parity plot of calculated and measured dimensionless pressure drops for data of Iliuta et al., including downflow and upflow arrangements and non-Newtonian liquids. Dashed lines correspond to ±30% relative errors.

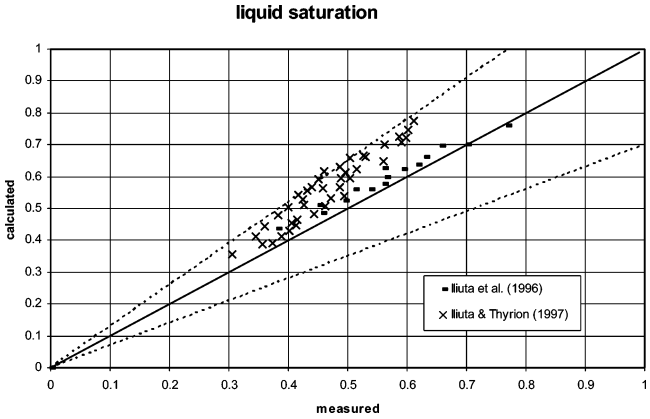

Figure 6. Parity plot of calculated and measured liquid saturations for data of Iliuta et al. Dashed lines correspond to ±30% relative errors.

for static holdup is required in the analysis. However, the value of static holdup may be important in the process design related to reactor startup and shutdown.

One parameter was re-fitted to the available data,[29−38] namely, the pulsing parameter (a_P). Its optimal value was determined to be 0.65. Parity plots of the predicted and measured dimensionless pressure drop and liquid saturation are shown in Figures 3 and 4. The so-called "low interaction regime" is reasonably well-predicted, as well as pulsing flow. About half of the data points lay in the pulsing region of the Charpentier plot.[39]

An interesting observation was made during the model analysis. In some occasions (∼15% of the data points), the model predicts multiple steady states for the gas holdup. The largest root (i.e., the largest gas saturation) was assumed to be the correct one, whereas the two other roots corresponded to cases where gas flows preferably along relatively straight paths in the particle interstices. The smaller gas saturation roots were also associated with lower pressure drops than in the base case. In the present analysis, the smallest roots were considered unstable. A geometric interpretation of the smallest roots would be a stable gas slug that does not collapse into separate bubbles even at low gas saturations. A detailed analysis of this model behavior is interesting and deserves further attention, but is left outside the scope of the present work. Despite the predicted multiple steady states in some cases, the model solution was relatively robust, and the correct root was found in almost every studied case, using a single initial gas saturation value of 0.5. The original slit model with constant Ergun parameters predicts multiple steady states as well, but less frequently than with the present model, because of a simpler gas saturation dependency.

The data of Iliuta et al.[30,31] consists of both downflow and upflow arrangements, and Newtonian as well as non-Newtonian liquids. Given that information, the predictions are surprisingly accurate (see Figures 5 and 6). It is also interesting that some data sets (e.g., the low-pressure data of Urseanu et al.[32]) are very well-predicted (see Figure 7), whereas some data sets show slightly increased scatter around the predicted mean[33,34] (see Figure 8); however, even for these data sets, there is no systematic error in the prediction.

Overall, the average relative errors were ∼30% for the pressure drop and ∼20% for the liquid holdup. Considering the hysteresis that is inherent to low flow rates, and, closely related to it, the effect of liquid pre-wetting, it is doubtful that any simple and truly predictive model could perform much better among the scattered data. Although the correlations could be improved by adding terms representing the direction of flow modulation, these are of not much practical benefit, because the catalyst life cycle in large-scale trickle-bed reactors should generally be on the order of years, and it is doubtful that any start-up modulation has an effect during a time period relevant in that time scale. A much more important feature is that the model predictions can be extended to flow conditions that were not precisely considered in the underlying physical model, which gives further confidence in the model application.

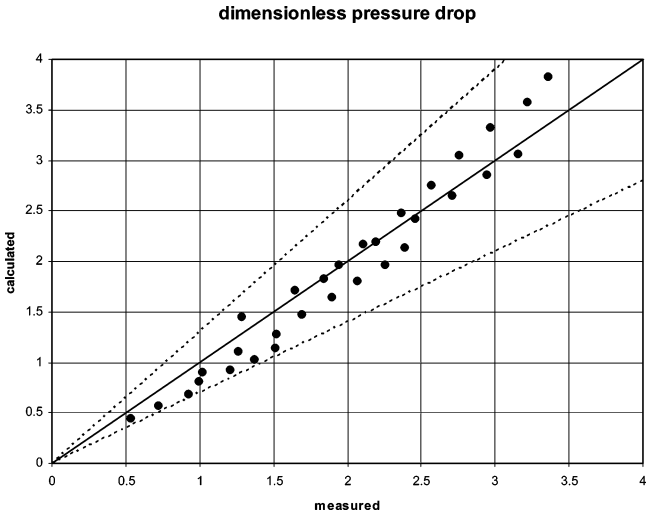

Figure 7. Parity plot of calculated and measured dimensionless pressure drops for data of Urseanu et al.[32] Dashed lines correspond to ±30% relative errors.

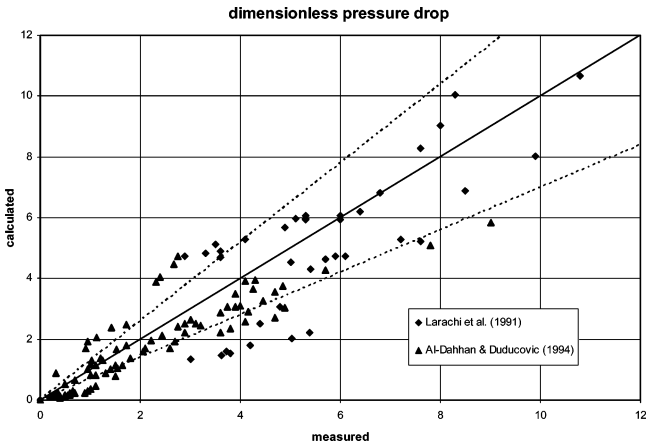

Figure 8. Parity plot of calculated and measured dimensionless pressure drops for data of Larachi et al.[34] and Al-Dahhan and Duducovic.[33] Dashed lines correspond to ±30% relative errors.

Conclusion

An algebraic model for estimating trickle-bed pressure drops and phase holdups was developed. The model is based on one-dimensional material and momentum balances for gas and liquid phases. Interaction models for gas−liquid and liquid−solid momentum transfer were considered, and physical reasoning was used to discard some of the previously developed models. New physical models were developed for the gas- and liquid-flow tortuosity, the capillary force effects, and for non-Newtonian fluids. Also, ,a gas density correction was proposed, which improves the accuracy of the algebraic approach, compared to its differential counterpart, mainly in cases where the pressure drop is considerable compared to the total pressure.

The developed model can be solved by one-parameter iteration. Both pressure drop and liquid holdup information is readily obtained from this solution. The model can be used without any extra complication in situations where the boundary conditions are specified, either at the inlet or at the outlet of the reactor. Because of the possibility to model a wide range of different interactions between the phases, it is suitable for modeling both low- and high-pressure operations, trickling as well as pulsing flow, upflow and downflow arrangements, and processes with Newtonian as well as non-Newtonian liquids.

In the numerical comparisons, the model predictions were first compared to its differential counterpart. The algebraic and differential model results were shown to be very close, giving confidence in using the simpler algebraic model. Finally, the model predictions were compared to available experimental data and other literature correlations. It was determined that the model predicts most datasets reasonably well, and, even more accurately, those datasets that are the most relevant for trickle-bed reactor operation.

Nomenclature

$\mathbf{A}$ = mass matrix (various)
A = viscous interaction parameter ($1/m^2$)
a_c = parameter in the capillary force correction
a_P = parameter in the pulsing flow correction to the tortuosity model
b = column matrix of source terms (various units)
B = inertial interaction parameter (1/m)
Ca = Capillary number; $Ca = \mu j/\epsilon\sigma$
d_p = particle diameter (m)
E = Ergun parameters
Eo^* = Modified Eötvös number; $Eo^* = \rho_L g d_p \epsilon^2/[\sigma(1-\epsilon)^2]$
F, f = momentum source terms based on bed void volume (N/m^3)
f_τ = friction factor
g = gravitational acceleration (m/s^2)
h = bed height (m)
j = superficial velocity (m/s)
k = viscosity model parameter (kg/ms)
Ka = Kapiza number; $Ka = \sigma^3\rho_L/(\mu_L{}^4 g)$
M = molar mass (kg/mol)
n = viscosity model parameter
P = pulsing parameter
p = pressure (Pa)
R = gas constant (J/(K mol))
$Re_{L,crit}$ = critical Reynolds number for pulsing; $Re_{L,crit} = \rho_L j_L d_p/[\mu_L(1-\epsilon)]$
T = temperature (K)
T = tortuosity
u_G = interstitial velocity of the gas phase (m/s)
u_L = interstitial velocity of the gas and liquid phase (m/s)
z = reactor bed height coordinate (m)
z_c = compressibility factor
a = gas interstitial volume fraction (gas saturation)
e = void fraction in bed
g = shear rate (1/s)
l = weighting factor in average density calculation
μ_G, μ_L = gas and liquid-phase viscosities (kg/ms)
q = angle of a slit
ρ_G, ρ_L = gas and liquid-phase densities (kg/m^3)
s = surface tension (N/m)
ξ_P = pulsing correction to liquid-phase tortuosity
Ψ_L = dimensionless liquid-phase body force; $\Psi_L = 1 - 1/(\rho_L g)(dp/dz)$

Literature Cited

(1) Jiang, Y.; Khadilkar, M. R.; Al-Dahhan, M. H.; Duduković, M. P. CFD of multiphase flow in packed-bed reactors: I. k-fluid modeling issues. *AIChE J.* **2002**, *48*, 701−715.

(2) Jiang, Y.; Khadilkar, M. R.; Al-Dahhan, M. H.; Duduković, M. P. CFD of multiphase flow in packed-bed reactors: II. results and applications. *AIChE J.* **2002**, *48*, 716−730.

(3) Nemec, D.; Levec, J. Flow through packed bed reactors: 2. Two-phase concurrent downflow. *Chem. Eng. Sci.* **2005**, *60*, 6958−6970.

(4) Drew, D. A. Mathematical modeling of two-phase flow. *Annu. Rev. Fluid Mech.* **1983**, *15*, 261−291.

(5) Iliuta, I.; Larachi, F. Modelling the hydrodynamics of gas−liquid packed beds via slit models: A review. *Int. J. Chem. React. Eng.* **2005**, *3*, Review R4.

(6) Souadnia, A.; Soltana, F.; Lesage, F.; Latifi, M. A. Some computational aspects in the simulation of hydrodynamics in a trickle-bed reactor. *Chem. Eng. Process.* **2005**, *44*, 847−854.

(7) Saez, A. E.; Carbonell, R. G. Hydrodynamic parameters for gas−liquid cocurrent flow in packed beds. *AIChE J.* **1985**, *31*, 52−62.

(8) Holub, R. A.; Duduković, M. P.; Ramachandran, P. A. A phenomenological model for pressure drop, liquid holdup, and flow regime transition in gas−liquid trickle flow. *Chem. Eng. Sci.* **1992**, *47*, 2343−2348.

(9) Tung, V. X.; Dhir, V. K. A hydrodynamic model for two-phase flow through porous media. *Int. J. Multiphase Flow* **1988**, *14*, 47−65.

(10) Attou, A.; Boyer, C.; Ferschneider, G. Modelling of the hydrodynamics of the cocurrent gas−liquid trickle flow through a trickle-bed reactor. *Chem. Eng. Sci.* **1999**, *54*, 785−802.

(11) Narasimhan, C. S. L.; Verma, R. P.; Kundu, A.; Nigam, K. D. P. Modeling hydrodynamics of trickle-bed reactors at high pressure. *AIChE J.* **2002**, *48*, 2459−2474.

(12) Iliuta, I.; Larachi, F. The generalized slit model: Pressure gradient, liquid holdup & wetting efficiency in gas−liquid trickle flow. *Chem. Eng. Sci.* **1999**, *54*, 5039−5045.

(13) Radilla, G.; Fourar, M.; Larachi, F. Correlating gas−liquid cocurrent flow hydrodynamics in packed beds using the F-function concept. *J. Chem. Technol. Biotechnol.* **2005**, *80*, 107−112.

(14) Ergun, S. Fluid flow through packed columns. *Chem. Eng. Prog.* **1952**, *48*, 89−94.

(15) Handley, D.; Heggs, P. J. Momentum and heat transfer mechanisms in regular shaped packings. *Trans. Inst. Chem. Eng.* **1968**, *46*, T251.

(16) Macdonald, I. F.; El-Sayed, M. S.; Mow, K.; Dullien, F. A. L. Flow through porous media−The Ergun equation revisited. *Ind. Eng. Chem. Fundam.* **1979**, *18*, 199−208.

(17) Al-Dahan, M. H.; Khadilkar, M. R.; Wu, Y.; Duduković, M. P. Prediction of pressure drop and liquid holdup in high-pressure trickle-bed reactors. *Ind. Eng. Chem. Res.* **1998**, *37*, 793−798.

(18) Iliuta, I.; Larachi, F.; Grandjean, B. P. A. Pressure drop and liquid holdup in trickle flow reactors: improved Ergun constants and slip correlations for the slit model. *Ind. Eng. Chem. Res.* **1998**, *37*, 4542−4550.

(19) Kundu, A.; Nigam, K. D. P.; Verma, R. P. Catalyst wetting characteristics in trickle-bed reactors. *AIChE J.* **2003**, *49*, 2253−2263.

(20) Nemec, D.; Levec, J. Flow through packed bed reactors: 1. Single-phase flow. *Chem. Eng. Sci.* **2005**, *60*, 6947−6957.

(21) Iliuta, I.; Larachi, F.; Al-Dahhan, M. H. Double-slit model for partially wetted trickle flow hydrodynamics. *AIChE J.* **2000**, *46*, 597−609.

(22) Holub, R. A. Hydrodynamics of trickle bed reactors, D.Sc. Thesis, Washington University, St. Louis, MO, 1990.

(23) Chatzis, I.; Morrow, N. R. Correlation of Capillary Number Relationships for Sandstone. *SPE J.* **1984**, (October), 555−562.

(24) Dullien, F. A. L. *Porous Media. Fluid Transport and Pore Structure*, 2nd Edition; Academic Press: San Diego, CA, 1992.

(25) Wang, R.; Mao, Z.-S.; Chen, J. Experimental and theoretical studies of pressure drop hysteresis in trickle bed reactors. *Chem. Eng. Sci.* **1995**, *50*, 2321−2328.

(26) Brodkey, R. S.; Hershey, H. C. *Transport Phenomena, a Unified Approach*; McGraw−Hill: New York, 1988.

(27) Larachi, F.; Iliuta, I.; Al-Dahhan, M. A.; Dudukovic, M. P. Discriminating trickle-flow hydrodynamic models: some recommendations. *Ind. Eng. Chem. Res.* **2000**, *39*, 554−556.

(28) Choudhary, M.; Propster, M.; Szekely, J. On the importance of the inertial terms in the modeling of flow maldistribution in packed beds. *AIChE J.* **1976**, *22*, 600−603.

(29) Clements, L. D.; Schmidt, P. C. Two-phase pressure drop in cocurrent downflow in packed beds: air-silicone oil systems. *AIChE J.* **1980**, *26*, 314−317.

(30) Iliuta, I.; Thyrion, F. C.; Muntean, O. Hydrodynamic characteristics of two-phase flow through fixed beds: air/Newtonian and non-Newtonian liquids. *Chem. Eng. Sci.* **1996**, *51*, 4987−4995.

(31) Iliuta, I.; Thyrion, F. C. Flow regimes, liquid holdups and two-phase pressure drop for two-phase cocurrent downflow and upflow through packed beds: air/Newtonian and non-Newtonian liquid systems. *Chem. Eng. Sci.* **1997**, *52*, 4045−4053.

(32) Urseanu, M. I.; Boelhouwer, J. G.; Bosman, H. J. M.; Schoijen, J. C.; Kwant, G. Estimation of trickle-to-pulse flow regime transition and pressure drop in high-pressure trickle bed reactors with organic liquids. *Chem. Eng. J.* **2005**, *111*, 5−11.

(33) Al-Dahhan, M. H.; Duduković, M. P. Pressure drop and liquid holdup in high-pressure trickle-bed reactors. *Chem. Eng. Sci.* **1994**, *49*, 5681−5698.

(34) Larachi, F.; Laurent, A.; Midoux, N. Wild, G. Experimental study of a trickle-bed reactor operating at high pressure: two-phase pressure drop and liquid saturation. *Chem. Eng. Sci.* **1991**, *46*, 1233−1246.

(35) Burghardt, A.; Bartelmus, G.; Jaroszynski, M.; Kolodziej, A. Hydrodynamics and mass transfer in a three-phase fixed-bed reactor with cocurrent gas−liquid downflow. *Chem. Eng. J.* **1995**, *58*, 83−99.

(36) Colombo, A. J.; Baldi, G.; Sicardi, S. Solid−liquid contacting effectiveness in trickle bed reactors. *Chem. Eng. Sci.* **1976**, *31*, 1101−1108.

(37) Specchia, V.; Baldi, G. Pressure drop and liquid holdup for two phase concurrent flow in packed beds. *Chem. Eng. Sci.* **1977**, *32*, 515−523.

(38) Wammes, W. J. A.; Middelkamp, J.; Huisman, W. J.; deBaas, C. M. Westerterp, K. R. Hydrodynamics in a Cocurrent Gas−Liquid Trickle Bed at Elevated Pressures. *AIChE J.* **1971**, *37*, 1849−1862.

(39) Charpentier, J.-C.; Favier, M. Some liquid holdup experimental data in trickle-bed reactors for foaming and nonfoaming hydrocarbons. *AIChE J.* **1975**, *21*, 1213−1218.

Received for review May 22, 2006
Accepted August 23, 2006

IE0606338